Dominik JURKÓW, Leszek GOLONKA

Faculty of Microsystem Electronics and Photonics, Wroclaw University of Technology

Application of mathematical statistic in preliminary investigations of high gauge factor thick film resistors

Streszczenie. *Technologie grubowarstwowa i niskotemperaturowej ceramiki współwypalanej znajdują zastosowanie w produkcji układów mikroelektronicznych, czujników, aktuatorów i mikrosystemów. Parametry układów wykonanych tymi technikami zależą w znacznej mierze od właściwości biernych elektronicznych elementów grubowarstwowych oraz dokładności procesu obróbki mechanicznej lub laserowej materiału. Z tego względu właściwości elementów biernych naniesionych na różne podłoża ceramiczne muszą być dokładnie analizowane. W pracy sprawdzono wpływ następujących parametrów: rodzaju niskotemperaturowej ceramiki współwypalanej (DP951, HL2000, Ceram Tape GC), konfiguracji rezystorów (zagrzebane, powierzchniowe), wymiarów geometrycznych rezystorów wykonanych z pasty ESL 3414-B-HBM na podstawowy parametr rezystorów (rezystancję na kwadrat i jej rozrzut). Analiza została wykonana z zastosowanie statystyki matematycznej w celu weryfikacji poprawności wyników. (**Zastosowanie statystyki matematycznej we wstępnej ocenie właściwości rezystorów grubowarstwowych o wysokim współczynniku czułości odkształceniowej**)*

Abstract*. Thick-film and Low Temperature Cofired Ceramics technologies are widely used in the microelectronics, sensors, actuators and microsystems. The parameters of the devices depend on the properties of thick-film components and the quality of 3D structures machining. Hence, the properties of the components must be carefully analysed. The influences of the following parameters: type of the substrates (DP 951, HL2000 and Ceram Tape GC), resistor configurations (surface and buried), resistor dimensions and state of LTCC tapes (fired and green state) on the properties of ESL 3414-B-HBM thick film high GF resistors have been investigated and discussed in this paper. The investigations were done using completely randomized design of the experiment with two input parameters and statistical analysis.*

Słowa kluczowe: LTCC, rezystor, warstwy grube, GF, sitodruk.
Keywords: LTCC, resistor, thick film, GF, screen printing.

Introduction

The Thick-film (TF) and Low Temperature Cofired Ceramics (LTCC) technologies have been applied in high density electronic packages for many years [1-2]. The main advantages of LTCC are good mechanical and electrical properties. The ceramics can be also easily machined in the green state. Therefore, the technique has been recently utilized in the fabrication of various sensors, actuators and microsystems [3]. The application of the LTCC in the pressure and acceleration sensors has been developed in the recent years [4-6]. One of the most popular pressure, force and acceleration measurement principles is piezoresistivity.

The parameters of the LTCC devices strongly depend on the properties of thick-film components. The thick-film pastes are dedicated to proper LTCC tapes. New applications demand sometimes pastes dedicated to other substrates (e.g. higher TCR or GF). The mismatch of the Coefficients of Thermal Expansion (CTE) between the LTCC and the thick film paste, different shrinkage coefficients and poor adhesion of the paste to the substrate are the main incompatibility problems. The generation of microcracks and increasing of the residual stress are directly connected with CTE mismatch. The shrinkage mismatch can generate structure deformations. The poor adhesion affects the stability of the thick film components. The chemical incompatibility problems may deteriorate both their basic electrical properties and stability. Therefore, the compatibility of LTCC tapes and the thick film pastes has to be analysed carefully before the fabrication of any novel devices [7-9].

The compatibility of ESL 3414-HBM thick film GF resistor with various LTCC tapes (DP 951, HL2000 and Ceram Tape GC) has been analysed and discussed in this paper. Moreover, the influences of the following parameters: resistor configurations (surface and buried) and the state of LTCC tapes (fired and green) on ESL 3414-HBM sheet resistance and variability coefficient have been analysed. The investigations were done using completely randomized design of the experiment with two input parameters and statistical analysis.

Experiment

The sheet resistance is assumed to be constant. However, for smaller resistors the sheet resistance depends on the component dimensions and normally decreases when the resistor dimensions decrease. The phenomenon is caused by metal migration from the electrodes into resistor and results in higher component thickness [10]. The sheet resistance is constant and does not depend on component's dimensions for bigger resistors. Therefore, the compatibility between thick film resistor and substrate, resistor configuration and firing type can be analysed using the test structure which consists of a matrix of resistors with different dimensions. If the sheet resistance does not depend on the components dimensions (for larger resistors) and the standard deviation is relatively low, it can be assumed that the resistor is compatible with the substrate, component configuration and firing type. The influence of resistor dimensions on the basic resistor parameters can be analysed using the test structure presented in Fig. 1.

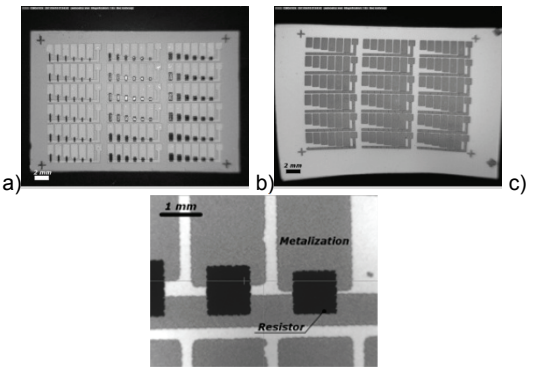

Fig. 1. Test structure, a) non deformed, b) deformed, c) screen printed resistors

Two test structures were fabricated for each tape, configuration and firing type. The single test structure consists of 108 resistors, divided into 18 groups (components length 0.2 – 1.4 mm, width 0.3 – 0.9 mm). Each group of components includes six resistors with the

same dimensions. Therefore, the sheet resistance of a single component was calculated as an average value of sheet resistance of 12 resistors. The used ESL 3414-B-HBM thick film resistor, according to the datasheet, has sheet resistance at alumina equal to 2.5-3.0 kΩ/□.

Results and discussion

The proper non deformed structure and the deformed one (mismatch of shrinkage coefficients between the substrate and the paste) are presented in Figs. 1a and 1b, respectively. The incompatibility between CeramTape and DP6146 PdAg paste was so big that it was impossible to prepare the test samples, hence, the resistors parameters have not been investigated. The planarity of the structure (CeramTape) can be improved using a loading during the sintering process. However, the method is useless if more complicated structures would be manufactured.

Generally, the sheet resistance does not depend on the resistor dimensions. However, in practice, the sheet resistance decreases when the resistor length decreases (for small components). The phenomenon is caused by higher impact of metals diffusion from the electrodes to the resistor during the firing. Moreover, shorter components are typically thicker in comparison with the longer ones. The variability coefficient decreases when the resistor surface area increases, which is connected with the printing accuracy. Larger resistors are easier to deposit and any inaccuracies during the screen printing process affect bigger resistors in a lower degree, in comparison with the smaller ones. Hence, the variability coefficient for the smaller resistors is significantly higher. The value of the variability coefficient should be as small as possible. Therefore, the resistors which have the variability coefficients higher than 15% are not recommended by the authors. The compatibility between a paste and a substrate can be assumed as good if the sheet resistance does not depend on the resistors dimensions or is stable above some level (e.g. for dimensions bigger than 0.5x0.5 mm) and the variability coefficient decreases when the component surface area increases. Otherwise, the components and substrate are not compatible. The printing quality is presented in Fig. 1c. The resistors edges are not smooth, the problem is caused by inaccuracy of the screen mask. The variability coefficient V has been calculated using equation 1 (where: □R – standard deviation, Ra – average sheet resistance).

$$V = \frac{\sigma_R}{R_a} \cdot 100\% \tag{1}$$

where: σ_R – standard deviation, R_a – average sheet resistance.

The highest incompatibility between the component and substrate occurred for the DP951 (buried configuration). All resistors were open circuited. Therefore, the results have not been included in the paper.

The influence of resistor dimensions, different LTCC tapes and resistors configurations on the sheet resistance and variability coefficient are presented in Figs. 2 and 3 (where: *R1*, *R2*, *R3* – average sheet resistance of 0.9, 0.6 and 0.3 mm wide resistors, respectively; *V1*, *V2*, *V3* – average variability coefficient of 0.9, 0.6 and 0.3 mm wide resistors, respectively). The analysis of the variances of examined combination of tape, firing and resistor configurations are presented in Tables 1 – 5 (where: *w* – resistor width, *l* – resistor length, *DF* – degrees of freedom, *SS* – square sum with correction, *F* – empiric value of Fisher-Snedecor coefficient, F_c – critical value of Fisher-Snedecor coefficient). The resistor width and length are input parameters. The square sum with correction is just an additional value demanded to calculate the empirical value of Fisher-Snedecor coefficient. It was included in all tables to simplify the calculations of *F* coefficient. The empirical and critical values of Fisher-Snedecor coefficient are necessary to make the assumption about compatibility or incompatibility between thick film resistor and substrate, component configuration or firing type.

Completely randomized design of the experiment with two input parameters was used to analyse statistically the influence of various described above parameters on the sheet resistance [11]. The statistical significance was set to 0.05, resistor length (*l*) and width (*w*) were set as input parameter 1 and 2, respectively. The average sheet resistances were calculated for rows ($\bar{R}_i$) and columns ($\bar{R}_j$). The empiric Fisher-Snedecor coefficient was calculated for parameters 1 and 2. The goal of the calculations was to find such combination of tape type, resistor configuration and firing which does not affect the sheet resistance in the investigated range. Exemplary calculations were presented in Appendix 1.

The behaviour of the variability coefficients for almost all examined structures are consistent with the theory and the coefficient decreases when the component dimensions increase. The analysis of the variances of all examined combinations of tape, firing and resistor configurations are presented in Tables 1 – 5. The Fisher-Snedecor *F* coefficient is higher than its critical value for at least one parameter in all examined combinations. Hence, the lack of compatibility can be inferred for all examined combinations. According to the analysis of the variances, the *F* coefficient is significantly higher for the resistors deposited on DP951 tape. Hence, the bigger incompatibility can be assumed for DP951 substrates. The components deposited on HL2000 tape (surface configuration, cofired) exhibit very low sheet resistance in comparison with other combinations. Hence, it would be very difficult to use such components as sensors.

The smallest changes in the sheet resistance vs. resistor dimensions exhibit the buried components inside HL2000 tape, according to Fig. 3a. Moreover, the *F* coefficient is the lowest one (Table 3) in comparison with other combinations. The resistors wider or equal to 0.6 mm are almost all stable and their sheet resistance does not depend on the resistor dimensions. The thesis can be proved using mathematical statistics. If calculations are carried out only for the components which are wider or equal to 0.6 mm, the estimated *F* coefficients are smaller than critical *F* value. The results of these calculations are presented in Table 6. Therefore, it can be assumed that the sheet resistance in this range does not depend on the resistor dimensions. Hence, the buried resistor configuration for HL2000 tape ensures the best properties of ESL 3414-HBM thick film GF resistors and is recommended by the authors. It must be borne in mind that not only the type of tape but also resistor configuration and type of firing affect properties of the resistors. The incompatibility can be assumed for surface components and compatibility can be inferred for buried components deposited on the same HL2000 tape.

The results achieved by the other researchers are presented in Tab.7. However, it has to be mentioned that the quoted authors used ESL 3414-B thick film paste, which according to the datasheet has different sheet resistance for alumina (3.6-4.4 kΩ/□**)** in comparison to the paste analysed in this paper **(**2.5-3.0 kΩ/□**).** Therefore, the literature and presented in this work sheet resistances cannot be compared directly. On the other hand it is quite easy to compare the changes in the sheet resistance vs. resistor dimensions. The reported resistors [8] deposited on DP951 (component dimension 1.6x1.6 mm), exhibit sheet

resistance approximately three times higher in comparison to the results achieved for smaller resistors (dimension 1x1 mm [7,9]) deposited on DP951. Hence, the assumption of incompatibility between DP951 and postfired ESL 3414 resistors can be inferred also in this case.

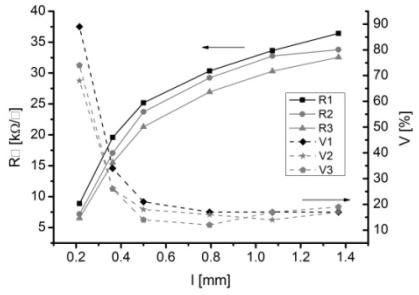

a)

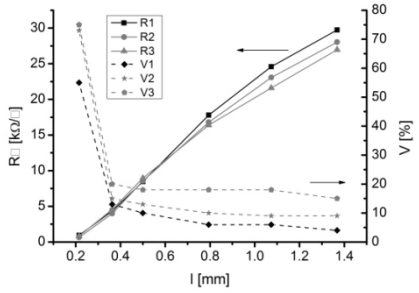

b)

Fig. 2. Sheet resistance and variability coefficient vs. resistor length, tape DP951 a) resistor configuration: surface, firing: postfiring, b) resistor configuration: surface, firing: cofiring.

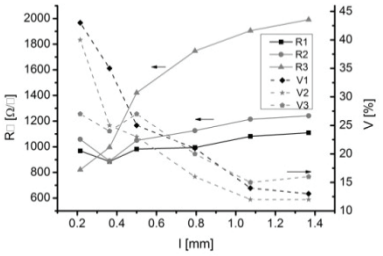

a)

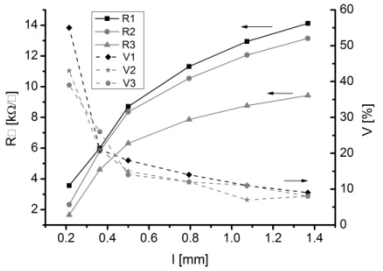

b)

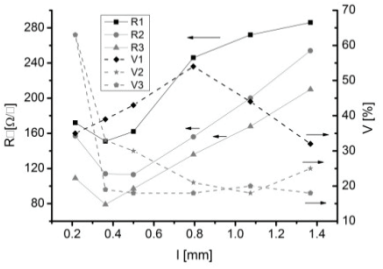

c)

Fig. 3. Sheet resistance and variability coefficient vs. resistor length, tape HL2000 a), resistor configuration: buried, firing: cofiring, b) resistor configuration: surface, firing: postfiring, c) resistor configuration: surface, firing: cofiring.

Table 1. Analysis of variances (tape: DP951, resistor configuration: surface, firing: postfiring).

Input parameter	*DF*	*SS* $[(\Omega/\square)^2]$	*F*	F_c
l	5	1508527797	1390.8028	3.3258
w	2	39327539	90.6461	4.1028
Error	10	2169291	-	-

Table 2. Analysis of variances (tape: DP951, resistor configuration: surface, firing: cofiring).

Input parameter	*DF*	*SS* $[(\Omega/\square)^2]$	*F*	F_c
l	5	1771191627	598.5368	3.3258
w	2	3810824	3.2195	4.1028
Error	10	5918405	-	-

Table. 3. Analysis of variances (tape: HL2000, resistor configuration: buried, firing: cofiring).

Input parameter	*DF*	*SS* $[(\Omega/\square)^2]$	*F*	F_c
l	5	1020474.05	4.4113	3.3258
w	2	702070.16	7.5873	4.1028
Error	10	462663.92	-	-

Table 4. Analysis of variances (tape: HL2000, resistor configuration: surface, firing: postfiring).

Input parameter	*DF*	*SS* $[(\Omega/\square)^2]$	*F*	F_c
l	5	205277109	75.1223	3.3258
w	2	29408500	26.9055	4.1028
Error	10	5465141	-	-

Table 5. Analysis of variances (tape: HL2000, resistor configuration: surface, firing: cofiring).

Input parameter	*DF*	*SS* $[(\Omega/\square)^2]$	*F*	F_c
l	5	42235	37.8670	3.3258
w	2	20421	45.7724	4.1028
Error	10	2231	-	-

Table. 6. Analysis of variances (tape: HL2000, resistor configuration: buried, firing: cofiring).
(range of resistor wide: 0.6 – 0.9 mm)

Input parameter	*DF*	*SS* $[(\Omega/\square)^2]$	*F*	F_c
l	5	233473	3.6347	5.0503
w	1	84481	6.5760	6.6079
Error	5	64235	-	-

Tab. 7. Literature data

Tape	Sheet resistance [kΩ/□]
DP951 postfired	64.8 [8], 22.6 [7,9]
DP951cofired	88.1 [8]

Conclusion

Completely randomized design of the experiment with two input parameters and statistical analysis was successfully applied in the investigation of compatibility between thick film resistors and substrates. The presented method is highly recommended for other researchers in such experiments.

The sheet resistance of the components deposited on DP951 (all configurations) and on HL2000 (only surface configuration) exhibits poor stability and changes drastically when the component dimensions change. Therefore, the lack of compatibility between DP951 and ESL 3414-B-HBM can be inferred.

The best results have been achieved for HL2000 tape, buried resistor configuration. According to the statistical calculations the variability coefficient is low and the sheet resistance is stable for the resistors wider or equal to 0.6 mm.

The tape type as well as resistor configuration and firing type affects the properties of resistors. The incompatibility can be assumed for surface components and compatibility can be inferred for buried components deposited on the same HL2000 tape.
The sheet resistances of ESL 3414 resistors deposited on DP951 reported in the literature depend also strongly on the component dimensions, hence, the lack of compatibility can be inferred in this case too.
The sheet resistance variability coefficient has to be decreased in the further research by improving screen printing accuracy.

Acknowledgments
The work has been financed by the Polish Ministry of Science and Higher Education in the years 2010-2012 as a research project (grant no. N N515 606839). Dominik Jurków fellowship financed by the Foundation for Polish Science (FNP).

Appendix Exemplary calculations [11] (tape: HL2000, resistor configuration: buried, firing of resistors: cofiring)
Statistical significance – 0.05
Input parameter 1 – resistor length
Input parameter 2 – resistor width

Table 8. Randomized experiment results (tape: HL2000, resistor configuration: buried, firing: cofiring)

l [mm]	*w* [mm]			$\bar{R}_i$
	0.3 mm	0.6 mm	0.9 mm	
0.3	821.35	895.28	968.13	894.92
0.45	995.65	970.19	885.60	950.48
0.6	1421.22	1106.39	981.90	1169.84
0.9	1747.03	1186.30	994.02	1309.12
1.2	1905.28	1385.83	1081.39	1457.50
1.5	1991.26	1483.64	1109.71	1528.20
$\bar{R}_j$	1480.30	1171.27	1003.46	$\bar{R} = \sum_{i=1}^{q} \bar{R}_i = \mathbf{1218.34}$

Calculation of average values of sheet resistance in table 8 rows ($\bar{R}_i$) and columns ($\bar{R}_j$)
Calculation of degrees of freedom for denominator (p i q – number of levels of variation for first and second input parameter)

$$f_2 = f_m = (p-1)(q-1) = (3-1)(6-1) = 10$$

Calculation of degrees of freedom of fraction for first parameter

$$f_{1I} = f_{lI} = (p-1) = (6-1) = 5$$

Calculation of degrees of freedom of fraction for second parameter

$$f_{1II} = f_{lII} = (q-1) = (3-1) = 2$$

Calculation of additional values

$$SS_I = q\sum_{i=1}^{p} \bar{R}_i^2 - pq\bar{R}^2 = 3(894.92^2 + \cdots + 1528.2^2) - 3 * 6 * 1218.34^2 = 1020474.05$$

$$SS_{II} = p\sum_{j=1}^{q} \bar{R}_j^2 - pq\bar{R}^2 = 702070.16$$

$$SS_R = \sum_{i=1}^{p}\sum_{j=1}^{q} R_{ij}^2 - q\sum_{i=1}^{p} \bar{R}_i^2 - p\sum_{j=1}^{q} \bar{y}_j^2 + pq\bar{R}^2 = 462663.92$$

Calculation of empirical F coefficient for first and second parameter:

$$F_I = \frac{S_I}{S_R}\frac{(p-1)(q-1)}{(p-1)} = 4.4113$$

$$F_{II} = \frac{S_{II}}{S_R}\frac{(p-1)(q-1)}{(q-1)} = 7.5873$$

Critical value of F coefficient:

$$F_{cI} = F_{(0,05;f_{1I};f_2)} = F_{(0,05;5;10)} = 3.3258$$

$$F_{cII} = F_{(0,05;f_{1II};f_2)} = F_{(0,05;2;10)} = 4.1028$$

Verification of empirical and critical values of F coefficient:

$$F_I > F_{cI}$$

$$F_{II} > F_{cII}$$

Therefore, it can be assume that the sheet resistance depends on both parameters.

Table 14. Analysis of variances

	DF	*SS* [(Ω/□)^2]	*F*	F_c
Parameter 1 (*l*)	p-1	$q\sum_{i=1}^{p} \bar{R}_i^2 - pq\bar{R}^2$	$\frac{S_I}{S_R}\frac{(p-1)(q-1)}{(p-1)}$	$F_{(0,05;f_{1I};f_2)}$
Parameter 2 (*w*)	q-1	$p\sum_{j=1}^{q} \bar{R}_j^2 - pq\bar{R}^2$	$\frac{S_{II}}{S_R}\frac{(p-1)(q-1)}{(q-1)}$	$F_{(0,05;f_{1II};f_2)}$
Error	(p-1) (q-1)	$\sum_{i=1}^{p}\sum_{j=1}^{q} R_{ij}^2 - q\sum_{i=1}^{p} \bar{R}_i^2 - p\sum_{j=1}^{q} \bar{y}_j^2 + pq\bar{R}^2$	-	-

REFERENCES

[1] Ibanez-Garcıa N., Martınez-Cisneros C.S., Valdes F., Alonso, J. Green-tape ceramics. New technological approach for integrating electronics and fluidics in microsystems, Trends in Analytical Chemistry(2008), n. 27, 24-33.
[2] Lahti M., Lantto V., Passive RF band-pass filters in an LTCC module made by fine-line thick-film pastes. Journal of the European Ceramic Society (2001), n. 21, 1997–2000
[3] Thelemann T., Thust H., Hintz M., Using LTCC for microsystems, Microelectronics International (2002), n. 19, 19–23
[4] Pietrikova A., Potentiality of LTCC for sensor applications. 24th International Spring Seminar on Electronics Technology (2001), 112-116.
[5] Zarnik M.S., Belavic D., Macek S., The warm-up and offset stability of a low-pressure piezoresistive ceramic pressure sensor, Sensors and Actuators A (2010), n. 158, 198–206.
[6] Neubert H., Partsch U., Fleischer D., Gruchow M., Kamusella A., Pham T., Thick film accelerometers in LTCC-technology – design optimization, fabrication, and characterization, Journal of Microelectronics and Electronic Packaging (2008), n. 5, 150-155.
[7] Hrovat M., Belavic D., Kita J., Holc J., Drnovsek S., Cilensek J., Thick-film strain and temperature sensors on LTCC substrates, Microelectronics International (2006), n. 23(3), 33–41
[8] Belavic D., Hrovat M., Holc J., Zarnik M.S. Kosec, M., Pavlin M. The application of thick-film technology in C-MEMS, Journal Electroceramics (2007), n. 19, 363–368.
[9] Hrovat M., Belavic D., Bencan A., Bernard J., Holc J., Cilenšek J., Smetana W., Homolka H., Reicher R., Golonka L., Dziedzic, A., Kita J., Thick-film resistors on various substrates as sensing elements for strain-gauge applications, Sensors and Actuators A (2003), n. 107, 261–272.
[10] Balik F., Golonka L., Jurewicz R., A comparison of thick-film resistor dimensional modeling methods, Proceedings of the 16-th conference of ISHM Poland (1992), Cracow, 71-74.
[11] Korzyński M., Experiment methodology. WNT(2006).

***Autorzy**: Dominik Jurków, dominik.jurkow@pwr.wroc.pl*
Leszek Golonka, leszek.golonka@pwr.wroc.pl
Wroclaw University of Technology, Faculty of Microsystem Electronics and Photonics, Wybrzeże Wyspiańskiego 27, 50-370 Wroclaw, Poland,